Journal of Microscopy, Vol. 176, Pt 3, December 1994, pp. 231–237.
Received 18 May 1994; accepted 23 September 1994

The tetrahedral tip as a probe for scanning near-field optical microscopy at 30 nm resolution

U. C. FISCHER, J. KOGLIN & H. FUCHS
Physikalisches Institut, Westfälische Wilhelms-Universität, Wilhelm Klemmstr. 10, 48149 Münster, Germany

Key words. Scanning near-field optical microscopy, scanning probe microscopy, evanescent waves, photon scanning tunnelling microscope, optical waveguides.

Summary

The tetrahedral tip is introduced as a new type of a probe for scanning near-field optical microscopy (SNOM). Probe fabrication, its integration into a scheme of an inverted photon scanning tunnelling microscope and imaging at 30 nm resolution are shown. A purely optical signal is used for feedback control of the distance of the scanning tip to the sample, thus avoiding a convolution of the SNOM image with other simultaneous imaging modes such as force microscopy. The advantages of this probe seem to be a very high efficiency and its potential for SNOM at high lateral resolution below 30 nm.

Introduction

In a transmission-type scanning near-field optical microscope (SNOM), a nanoscopic tip serves as a light-emitting antenna. It is excited by light from a source via an optical path or by a waveguide such as a glass fibre and a link which transmits light between the macroscopic waveguide and the tip, as shown schematically in Fig. 1.

Light emitted from the tip and transmitted through the object is directed to a detector and converted into an electrical signal which is used for imaging. The tip and the link have specific near-field optical functions and therefore are the characteristic parts of a near-field optical microscope.

Tapered, metal-clad monomode fibres ending in a tip with an aperture 10–100 nm in diameter at its apex are very successfully used as probes for SNOM (Betzig & Trautman, 1992). The metal-clad conical taper constitutes in this case the link between the fibre and the aperture. This link is expected to be a rather inefficient one due to severe cut-off in regions where the cone diameter is significantly smaller than the wavelength of the transmitted light (Roberts, 1991).

The concept of the coaxial tip (Fee *et al.*, 1989; Fischer & Zapletal, 1991; Keilmann & Merz, 1993) with an additional conical metal core tries to overcome this limitation based on the model of such a tip – assuming an ideally conducting metal – which supports a TEM (transverse electric and magnetic) mode without cut-off, and which in principle allows electromagnetic energy to be focused to dimensions which are small compared with the wavelength. There has been an attempt to realize this concept for optical frequencies (Fischer & Zapletal, 1991), but a satisfactory fabrication scheme has not yet been found. Similar considerations lead us to the concept of the tetrahedral tip (Danzebrink & Fischer, 1993; Fischer, 1993a,b).

The concept of the tetrahedral tip

A tetrahedral tip is shown schematically in Fig. 2. The body consists of a transparent material such as glass. It has three faces and edges which converge to a common tip. Two adjacent faces are coated with a thin film of metal, leaving the edge between the metal films free. The third face and the tip are also coated with metal.

For metals such as silver or gold, it is expected that propagating resonant surface plasmons can be excited in the visible spectral range either on the planar metal films or along the edge, in analogy to surface plasmon modes on cylindrical wires (Ruppin, 1982) and that a localized plasmon can be emitted from the tip. The excitation of surface plasmons on the metal faces is possible – in analogy to the Kretschmann configuration for exciting surface plasmons on thin metal films by attenuated total internal reflection (Raether, 1988) – by irradiating the metal films from within with a monochromatic beam of light at a selected angle to the metal coatings.

These surface waves may serve to transmit electromagnetic energy efficiently to the tip, from where they are emitted as radiation in non-specular directions. A resonant field enhancement due to coupled surface plasmon modes of the metal films and of the edge, and of local surface plasmon modes of the tip, may additionally lead to a strong field enhancement at the tip, as with protrusions from a gold

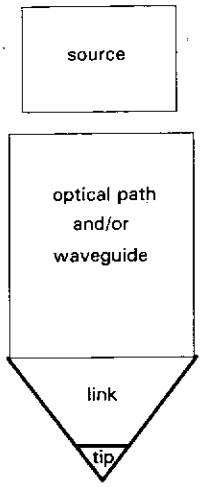

Fig. 1. Optical path for excitation of the emitting tip in a transmission-type SNOM.

film (Fischer & Pohl, 1989). The emitting tip serves as an SNOM probe.

Fabrication of tips

A simple, well-established laboratory scale technique is adopted for fabricating tetrahedral tips (Fischer, 1993a,b). Ultramicrotome glass blades for cutting thin sections of embedded biological material of a thickness down to 30 nm are routinely made by biologists. They are fabricated by cleaving a rectangular slab of glass twice at an angle.

A glass fragment of triangular cross-section as shown schematically in Fig. 3(a) is obtained with the K1 edge between the two newly formed fracture planes serving as a knife. The method can easily be modified to make the edge end in an equally well-defined corner, as shown in Fig. 4. This corner serves as the body of the tetrahedral tip. The two freshly formed fracture faces can be coated consecutively with approximately 50 nm of gold at an oblique angle relative to the edge, leaving the edge uncoated. The high resistance between the metal films indicates that they are truly separated (Danzebrink & Fischer, 1993). The fabrication scheme was scaled down to be applied to microscope cover glasses of 180 μm thickness instead of the rather bulky glass slabs commonly used for the fabrication of ultramicrotome knives. In addition, the metal coating conditions were modified such that the K2 and K3 edges, the face S23 and presumably also the tip itself were coated by exposing face S23 to the metal vapour beam. The glass fragment is attached to a small glass prism, as shown schematically in Fig. 3(b). In this way it is possible to irradiate the tetrahedral tip from within by a slightly focused beam of light which is inclined at an angle of approximately 45° to the edge.

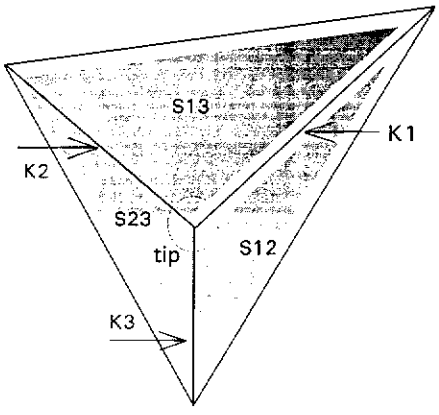

Fig. 2. Schematic view of the tetrahedral tip with three edges K1–3 and three faces S12, S13 and S23 converging to a common tip. All three faces are coated with a thin film of metal. K1 is not coated.

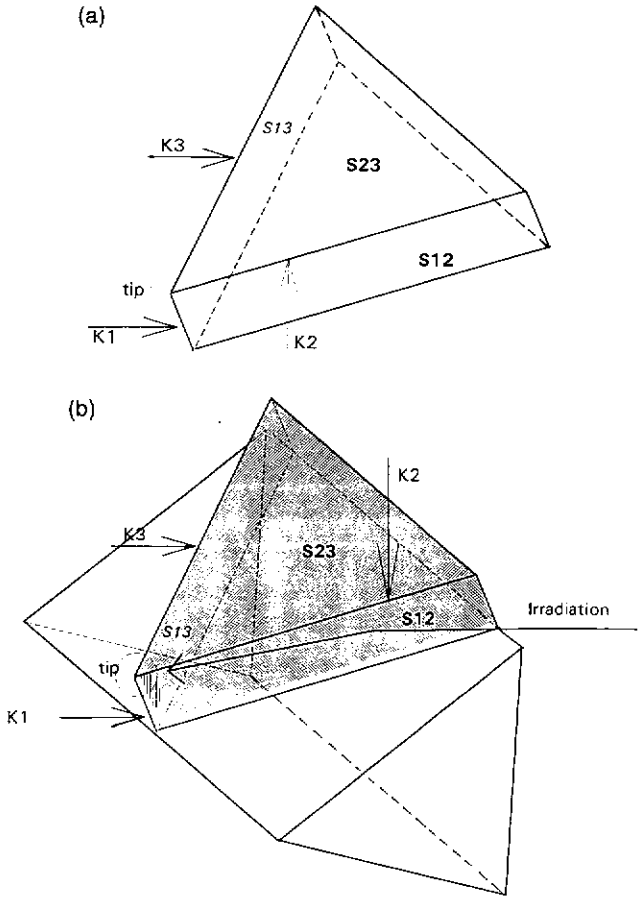

Fig. 3. (a) Schematic view of a glass fragment of triangular cross-section. (b) Glass fragment with metal-coated faces mounted on a prism.

The inverted photon scanning tunnelling microscope configuration

The tetrahedral tip is used as a nanoscopic light source for SNOM in an inverted photon scanning tunnelling micro-

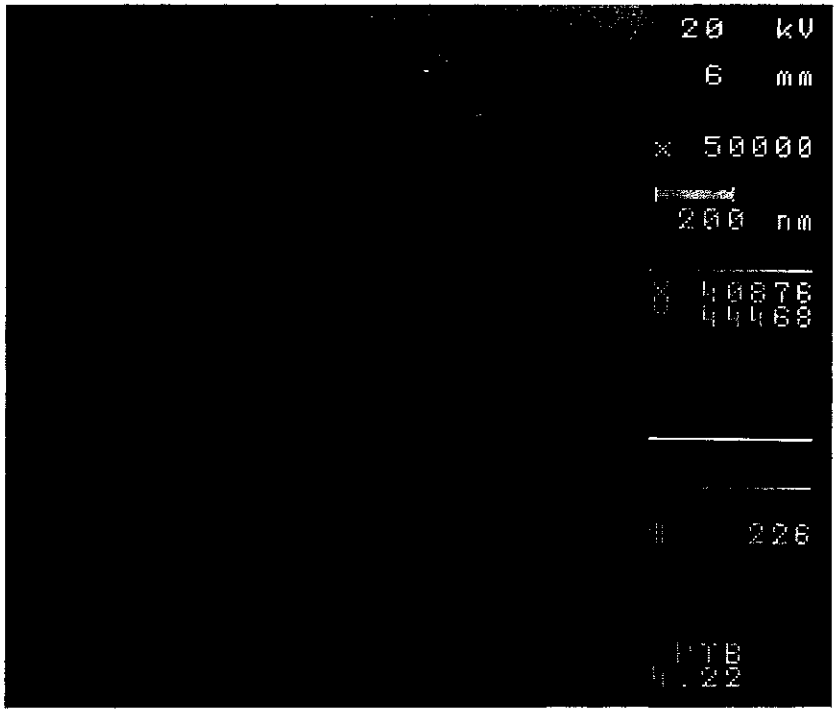

Fig. 4. SEM micrograph of the tetrahedral tip (gold sputtered).

scope configuration (Fischer & Zapletal, 1991; Fischer, 1993a,b; Hecht *et al.*, 1993), as shown schematically in Fig. 5(a).

A parabolic mirror filled with a transparent epoxy resin serves as a darkfield immersion collector of light emitted from the tip, as described below. The sample is a thin transparent film on a cover glass which is attached to the mirror by oil immersion. The central part of the other side of the mirror is covered by an opaque beam stop. The parabolic mirror serves as a valve to transmit light only if the tip penetrates into the range of the evanescent modes of the glass–air interface. When the tip is distant from the sample, light emitted from the tip is diffracted into the parabolic mirror only in the range of angles smaller than the angles of total internal reflection. This radiation is absorbed by the beam stop.

As the tip penetrates into the range of the evanescent modes, light emitted from the tip is diffracted into the angular range of total internal reflection (see e.g. Carniglia *et al.*, 1972). This set-up is part of the microscope shown schematically in Fig. 5(b).

The tip is irradiated by projecting into the tip a fourfold demagnified image of a 20-μm pinhole, which itself is irradiated by a focused beam of light of 632 nm from an HeNe laser. The parabolic mirror including the probe is mounted on a three-dimensional (3-D) coarse positioning element and on a 3-D Piezo scanner. The tip is mounted on a z-piezo element. A silicon photodiode is used to collect the light which is transmitted through the darkfield collector. A polarizer is inserted into the beam path in front of the tip and an analyser is inserted behind the collector. The irradiating beam is polarized in the y-direction and to a small extent in the z-direction due to the conical shape of the beam. The orientation of the K1 edge is also within the yz plane, as shown in Fig. 6(a) in a topview onto the tip.

We assume that radiation is emitted from the tip as result of an electrical dipole type of excitation with components orientated along the y- and z-axes. The polarization of light emitted from this z-component has a component orientated radially within the xy-plane and a z-component. After transmission through the darkfield collector the polarization will therefore be orientated radially in the xy-plane, as shown in Fig. 6(b). The light emitted in the y-direction will be y-polarized after reflection from the parabolic mirror, and light emitted in the x-direction will be converted to x-polarized light. Light emitted from the y-orientated dipole is polarized in the y-direction and retains this polarization after transmission through the darkfield collector. Adjusting the analyser to the x-direction, vertically to the polarization of the incident beam and to the K1 edge therefore selects radiation originating from the z-orientated dipole. Figure 7 shows the exponential increase of the detected signal as the tip approaches the surface of the sample.

The approach is stopped when the signal reaches a given value by means of a feedback loop. The feedback loop is used to perform scans in an apparently constant intensity mode similar to that used in scanning tunnelling microscopy. During a scan in the x–y-directions the tip is adjusted by means of the z-piezo element such that the detected signal remains constant. The z-signal which is fed into the z-piezo element is used to obtain a pseudo-topography of the object.

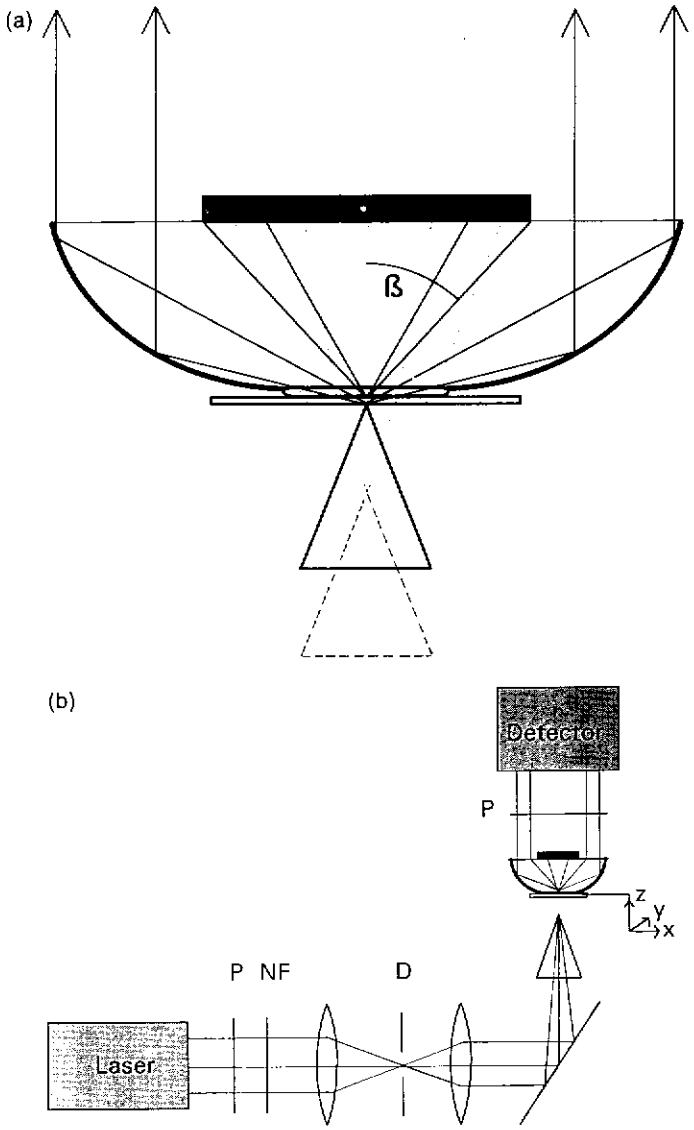

Fig. 5. (a) Schematic view of the darkfield immersion collector with the epoxy-filled parabolic mirror, beam stop, and cover glass attached by immersion oil. Light emitted from the tip passes through the collector only if the tip penetrates into the range of the evanescent modes of the glass–air interface. (b) Schematic view of the optical path of the inverted PSTM. P, polarizing filter; NF, neutral glass filter; D, diaphragm.

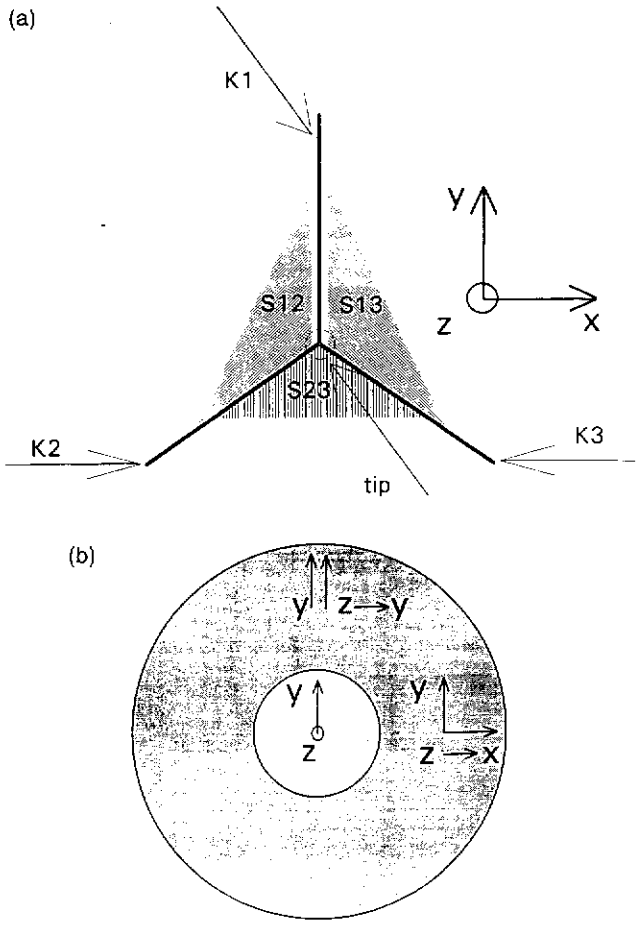

Fig. 6. (a) Schematic view of polarization of the incident beam with respect to the position of the tip as seen from above the tip. The polarization of the incident beam has its main component in the y-direction and a smaller component in the z-direction. (b) Schematic view of polarization of light transmitted through the immersion darkfield collector as seen from above the collector. y-Polarized emission from the tip retains the y-polarization after passage through the collector whereas emission from a z-polarized dipole is converted to a component polarized radially within the x–y plane after reflection by the parabolic mirror of the darkfield collector: z-polarized light emitted in the y-direction is converted to y-polarized light and z-polarized light emitted in the x-direction is converted to x-polarized light. Setting the analyser in the x-direction, only light originating from the z-orientated dipole will therefore be detected.

Imaging of latex projection patterns by SNOM

Latex projection patterns were fabricated by the method of 'natural lithography' as objects suitable to test the lateral resolution of imaging (Fischer & Zingsheim, 1981; Deckman & Dunsmuir, 1982). An AFM image of such an object consisting of an SiO_2 pattern on glass is shown in Fig. 8.

A hexagonally close packed monolayer of latex spheres 0·22 μm in diameter served as a mask for evaporation of a 25-nm-thick layer of SiO_2. The latex spheres were subsequently removed. Triangular patches c. 25 nm in height with curved baselines 30–100 nm long and with a centre to centre distance of 126 nm are formed as a projection of the interstices between the latex spheres. In the AFM image most, but not all, of these details are resolved. The triangular form of the patches is not resolved; they seem to be of a rather rectangular shape. It was shown previously by transmission electron microscopy that triangles are formed, the tips of the triangles having a radius of curvature of the order of 5 nm (Fischer &

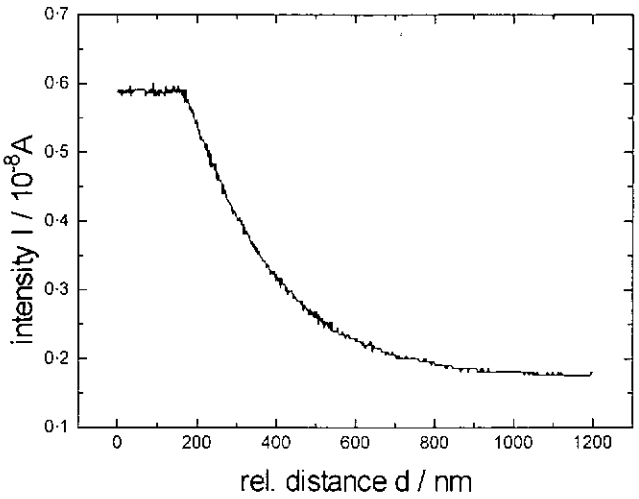

Fig. 7. Optical signal as a function of tip displacement towards the sample. The absolute distance between tip and sample is not known. The approach is stopped by means of a feedback loop when a set value of the signal is reached. In this experiment the feedback loop activates a piezoelement which retracts the sample to the same extent as the tip is advanced. Therefore, no further change of signal is obtained.

Zingsheim, 1981). The rectangular form of the patches in the AFM image is likely to be due to the probing tip which has a pyramidal shape and therefore a quadratic cross-section. The convolution of tip structure and the form of the patches is therefore likely to be the cause of the rectangular shape of the patches in the AFM image.

Better resolved AFM images may be obtained using other tip shapes. An SNOM image of the test structure is shown in Fig. 9(a). A standing-wave-like structure with a periodicity of *c.* 0·3 μm dominates the unfiltered image. In the upper left corner of the image there is, however, a clear indication of a hexagon of six patches. The hexagonal array of patches is clearly revealed after highpass filtering, as shown in Fig. 9(b). Taking another image at a different part of the same sample with the same tip gave us a much better resolved image of the test structure (Fig. 9c). The 126-nm centre to centre distance of the patches is again clearly resolved. The size of the patches in the range 30–100 nm is also correctly represented in the image. In addition there is a clear indication of the triangular form of the patches, as shown in Fig. 9(d), a magnified section of Fig. 9(c). The orientation of the triangles is different for the two examples shown. Therefore, we conclude that the triangular form of the patches is not caused by the triangular cross-section of the probing tip. A resolution well below 30 nm can therefore be inferred from the SNOM images shown.

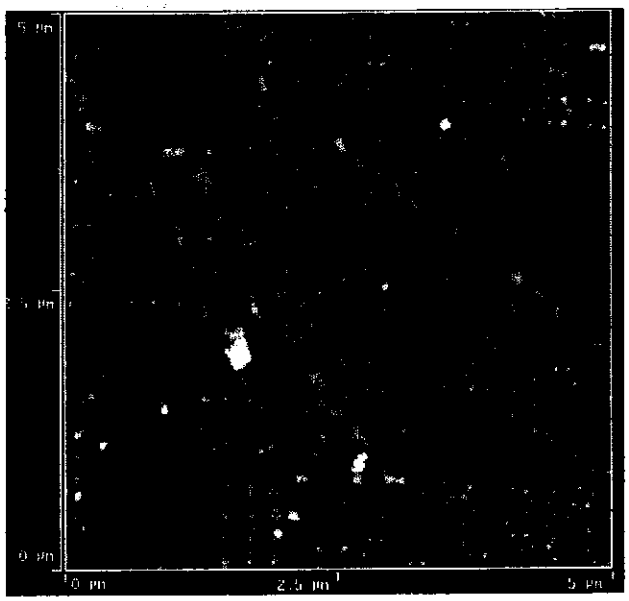

Fig. 8. AFM image of latex projection test patterns obtained from a mask consisting of a hexagonal array of 0·22-μm spheres.

Images were taken at a very slow scan speed because of the low mechanical resonances of our improvized mechanical set-up. There is still interference in the form of a 50-Hz vibration of small apparent spatial periodicity (of the order of 20 nm) seen in Fig. 9(d), which was found to be due to mechanical interference at 50 Hz.

Discussion

The images obtained with the SNOM appear as a superposition of a wavelike structure of a periodicity of *c.* 0·3 μm corresponding to approximately half the wavelength of the light from the HeNe laser, and a much better resolved structure at selected areas. We assume that the varying resolution is due to the optical feedback. The optical signal may not only depend on the distance between the tip and the sample but also on other factors, which still have to be explored.

The origin of the superimposed wavelike structure is not clear at present. It clearly does not represent a periodic modulation of the topography, because it is absent in the AFM images. It must be due to either optical properties of the emitting tip or to the detection pathway. A poorly defined local emitter consisting of a very localized area and an area with less well-defined emission may be the cause of an interference pattern. Alternatively, we may assume that even a well-localized emitting tip excites standing waves, which are connected to inhomogeneities in the surface of the sample.

From the images shown in Fig. 9(c,d) we conclude that SNOM with the tetrahedral tip as a probe has a potential resolution well below 30 nm. The demonstrated resolution is entirely due to optical image formation without any interference from a simultaneous force microscopic feedback system. The demonstrated resolution is still limited by mechanical interference as well as by the nature of the test

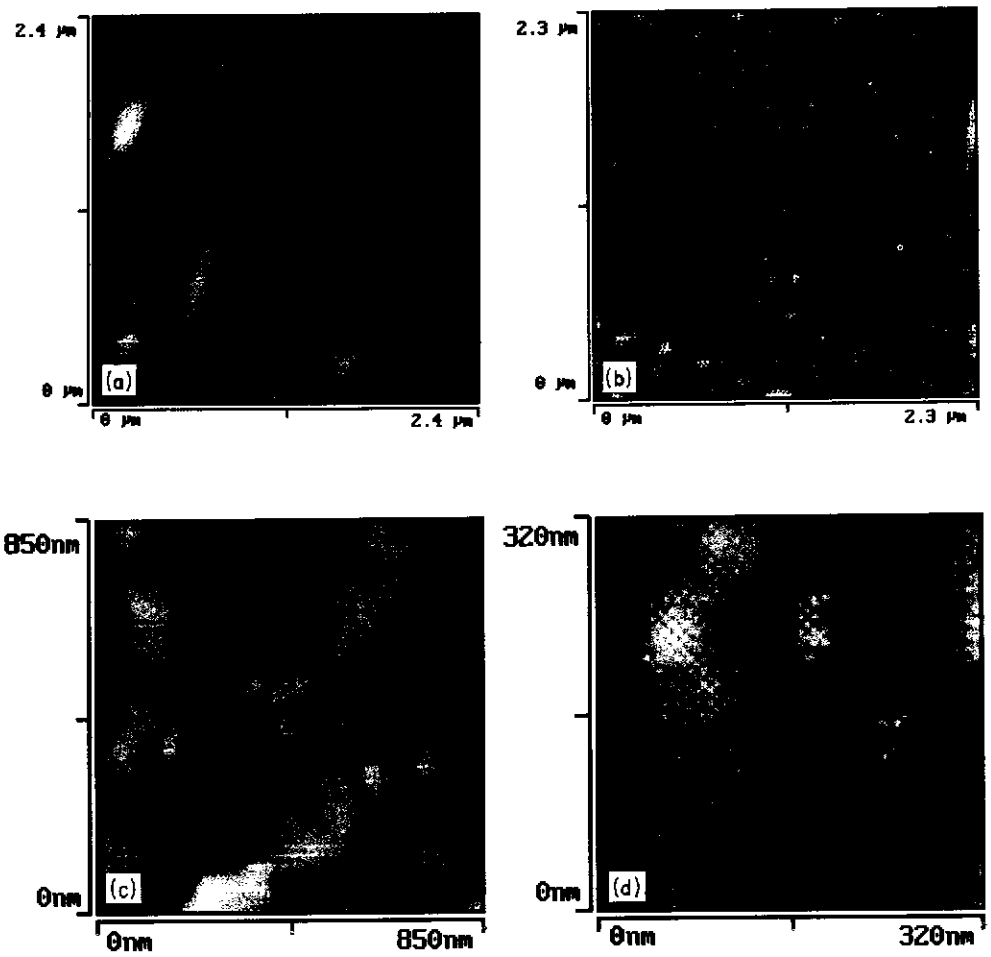

Fig. 9. (a) SNOM image of the same latex projection test pattern as in Fig. 8 (raw data); (b) same data after high-pass filtering; (c) SNOM image taken with the same tip at a different place (raw data); (d) magnified section of Fig. 9(c).

object. The patches are about 25 nm in height, so we would not expect that the resolution could be improved with a tip which has a rather wide opening angle. A more shallow test structure has to be chosen for a test of still higher resolution.

The tetrahedral tip seems to be a rather efficient probe. A silicon photodiode was sensitive enough to record an image at a resolution of 30 nm. The efficiency of the tip can be estimated. The detected signal corresponded to a fraction of at least 10^{-5} of the total light irradiating the tip, as determined by the respective relative signals measured with the photodiode. The irradiating light illuminates a circular area of 5 μm diameter within the tip of the demagnified image of the 20-μm aperture in the irradiating beam (see Fig. 5b). With the ratio of the apparent area ($2{\cdot}8 \times 10^{-3}$ μm^2) of the aperture of the tip – as estimated from the obtained resolution of 30 nm – to the total illuminated area (78 μm^2) within the tip, we estimate the apparent aperture of the tip to be irradiated with a fraction of $3{\cdot}5 \times 10^{-5}$ of the total intensity and that a fraction of 0·28 of this intensity is transmitted through the apparent aperture of the tip. This transmission factor of 0·28 is surprisingly high and should be compared with the theoretical values of transmission factors for apertures in a metal film, which decrease with the fourth power of the radius when the diameter is small compared with the wavelength. We therefore conclude that the tetrahedral tip fulfils the function of a link transmitting light very efficiently to nanoscopic dimensions.

The tetrahedral tip allows high-resolution SNOM in the 50–10-nm range. The high yield will allow us to explore the resolution limits of the probe. To explore the specific advantages of this new SNOM method versus AFM methods, which are better suited to the investigation of surface relief structures, and other SNOM methods, we need structures which are not just relief structures.

Acknowledgments

We thank Lifeng Chi and Boris Anczykowski for taking the AFM images of the latex projection patterns. U.C.F. acknowledges W. Mirandé for support in the initial stages

of the work and for stimulating discussions. This work was supported by the Deutsche Forschungsgemeinschaft and partly also by the Volkswagen foundation.

References

Betzig E. & Trautman, J.K. (1992) Near-field optics: microscopy beyond the diffraction limit. *Science*, **257**, 189–195.

Carniglia, C.K., Mandel, L. & Drexhage, K.H. (1972) Absorption and emission of evanescent photons. *J. Opt. Soc. Am.* **62**, 479–486.

Danzebrink, H.U. & Fischer, U.C.(1993) The concept of an optoelectronic probe for near field microscopy. *Near Field Optics* (ed. by D. W. Pohl and D. Courjon), pp. 303–308. Kluwer Academic Publ., the Netherlands.

Deckman, H.W. & Dunsmuir, J.H. (1982) Natural lithography. *Appl. Phys. Lett.* **41**, 377–379.

Fee M., Chu, S. & Hänsch, T.W. (1989) Scanning electromagnetic transmission line microscope with sub- wavelength resolution. *Opt. Commun.* **69**, 219–224.

Fischer, U.C. & Zingsheim, H.P. (1981) Submicroscopic pattern replication with visible light. *J. Vac. Sci. Technol.* **19**, 881–885.

Fischer, U.C. & Pohl D.W. (1989) Observation of single particle plasmons by near-field optical microscopy. *Phys. Rev. Lett.* **62**, 458–461.

Fischer, U.C. & Zapletal, M. (1991) The concept of the coaxial tip as a probe for scanning near field optical microscopy and steps towards a realisation. *Ultramicroscopy*, **42–44**, 393–398.

Fischer U.C. & Mirandé, W. (1993) Die Tetraederspitze als Sonde für die optische Nahfeldmikroskopie. *Abstracts of the 94th annual conference of the 'Deutsche Gesellschaft für angewandte Optik', Wetzlar June 1–5*, p. 14.

Fischer, U.C. (1993a) Probes for scanning near field optical microscopy (SNOM) and their modes of operation *Optik*, **94**, Suppl. 5 20.

Fischer, U.C. (1993b) The tetrahedral tip as a probe for scanning near-field optical microscopy. *Near Field Optics* (ed. by D. W. Pohl and D. Courjon), pp. 255–262. Kluwer Academic Publ., the Netherlands.

Hecht, B., Heinzelmann, H. & Pohl, D.W. (1993) Combined aperture SNOM/PSTM: best of both worlds? *Ultramicroscopy* (in press).

Keilmann, F. & Merz, R. (1993) Far-infrared near-field spectroscopy of two-dimensional electron systems. *Near Field Optics* (ed. by D. W. Pohl and D. Courjon), pp. 317–327. Kluwer Academic Publ., the Netherlands.

Raether, H. (1988) Surface plasmons on smooth and rough surfaces and on gratings. *Springer Tracts in Modern Physics 111* (ed. by G. Höhler), Springer, Berlin.

Roberts, A. (1991) Field detection by subwavelength aperture probes. *SPIE*, **1556**, 11–18.

Ruppin, R. (1982) Spherical and cylindrical surface polaritons in solids. *Electromagnetic Surface Modes* (ed. by A. D. Boardman), pp. 345–397. John Wiley & Sons Ltd.